J|A|C|S ARTICLES

Published on Web 10/20/2010

Disparate Effects of Cu and V on Structures of Exohedral Transition Metal-Doped Silicon Clusters: A Combined Far-Infrared Spectroscopic and Computational Study

Vu Thi Ngan,[†,§] Philipp Gruene,[||] Pieterjan Claes,[‡,§] Ewald Janssens,[‡,§] André Fielicke,*[,||] Minh Tho Nguyen,*[,†,§] and Peter Lievens*[,‡,§]

Department of Chemistry, Katholieke Universiteit Leuven, B-3001 Leuven, Belgium, Laboratory of Solid State Physics and Magnetism, Katholieke Universiteit Leuven, B-3001 Leuven, Belgium, Institute for Nanoscale Physics and Chemistry (INPAC), Katholieke Universiteit Leuven, B-3001 Leuven, Belgium, and Fritz-Haber-Institut der Max-Planck-Gesellschaft, Faradayweg 4-6, D-14195 Berlin, Germany

Received June 11, 2010; E-mail: fielicke@fhi-berlin.mpg.de; minh.nguyen@chem.kuleuven.be; peter.lievens@fys.kuleuven.be

Abstract: The growth mechanisms of small cationic silicon clusters containing up to 11 Si atoms, exohedrally doped by V and Cu atoms, are described. We find that as dopants, V and Cu follow two different paths: while V prefers substitution of a silicon atom in a highly coordinated position of the cationic bare silicon clusters, Cu favors adsorption to the neutral or cationic bare clusters in a lower coordination site. The different behavior of the two transition metals becomes evident in the structures of Si_nM^+ ($n = 4-11$ for M = V, and $n = 6-11$ for M = Cu), which are investigated by density functional theory and, for several sizes, confirmed by comparison with their experimental vibrational spectra. The spectra are measured on the corresponding $Si_nM^+ \cdot Ar$ complexes, which can be formed for the exohedrally doped silicon clusters. The comparison between experimental and calculated spectra indicates that the BP86 functional is suitable to predict far-infrared spectra of these clusters. In most cases, the calculated infrared spectrum of the lowest-lying isomer fits well with the experiment, even when various isomers and different electronic states are close in energy. However, in a few cases, namely Si_9Cu^+, $Si_{11}Cu^+$, and $Si_{10}V^+$, the experimentally verified isomers are not the lowest in energy according to the density functional theory calculations, but their structures still follow the described growth mechanism. The different growth patterns of the two series of doped Si clusters reflect the role of the transition metal's 3d orbitals in the binding of the dopant atoms.

1. Introduction

Silicon-based clusters have attracted continuous attention due to numerous technological applications of silicon and ongoing efforts to reduce sizes of silicon structures in nanomaterial research. In the past years, the need to miniaturize electronic devices has greatly stimulated the study of small silicon clusters containing up to 100 atoms.[1−13] Unlike carbon clusters that, for certain sizes, possess high stability with highly symmetric trivalent, i.e., sp^2 hybridized, carbon atoms, silicon clusters tend to adopt prolate structures, due to a high reactivity of the dangling bonds.[7]

It is well-known that the geometrical structures and chemical reactivities of clusters can significantly be changed upon appropriate doping.[14] For various clusters of different elements, transition metals turn out to be fascinating dopants due to their flexibility in forming new bonds. For silicon clusters, doping can lead to the formation of stable and unreactive cages of high symmetry,[15] which would be of utmost importance as possible building blocks in nanotechnological devices.

Following the first experimental realization of transition metal-doped silicon clusters by Beck, his discovery of magic numbers for specific sizes, and the subsequent proposition of

[†] Department of Chemistry, Katholieke Universiteit Leuven.
[§] Institute for Nanoscale Physics and Chemistry (INPAC), Katholieke Universiteit Leuven.
[||] Fritz-Haber-Institut der Max-Planck-Gesellschaft.
[‡] Laboratory of Solid State Physics and Magnetism, Katholieke Universiteit Leuven.

(1) Raghavachari, K.; Logovinsky, V. *Phys. Rev. Lett.* **1985**, *55*, 2853.
(2) Pacchioni, G.; Koutecký, J. *J. Chem. Phys.* **1986**, *84*, 3301.
(3) Brown, W. L.; Freeman, R. R.; Raghavachari, K.; Schluter, M. *Science* **1987**, *235*, 860.
(4) Cheshnovsky, O.; Yang, S. H.; Pettiette, C. L.; Craycraft, M. J.; Liu, Y.; Smalley, R. E. *Chem. Phys. Lett.* **1987**, *138*, 119.
(5) Jarrold, M. F. *Science* **1991**, *252*, 1085.
(6) Honea, E. C.; Ogura, A.; Murray, C. A.; Raghavachari, K.; Sprenger, W. O.; Jarrold, M. F.; Brown, W. L. *Nature* **1993**, *366*, 42.
(7) Röthlisberger, U.; Andreoni, W.; Parrinello, M. *Phys. Rev. Lett.* **1994**, *72*, 665.
(8) Li, S.; Van Zee, R. J.; Weltner, W., Jr.; Raghvachari, K. *Chem. Phys. Lett.* **1995**, *243*, 275.
(9) Ho, K.-M.; Shvartsburg, A. A.; Pan, B.; Lu, Z.-Y.; Wang, C.-Z.; Wacker, J. G.; Fye, J. L.; Brown, W. L. *Nature* **1998**, *392*, 582.
(10) Shvartsburg, A. A.; Liu, B.; Jarrold, M. F.; Ho, K.-M. *J. Chem. Phys.* **2000**, *112*, 4517.
(11) Zhu, X.; Zeng, X. C. *J. Chem. Phys.* **2003**, *118*, 3558.
(12) Nigam, S.; Majumder, C.; Kulshreshtha, S. K. *J. Chem. Phys.* **2004**, *121*, 7756.
(13) Hellmann, W.; Hennig, R. G.; Goedecker, S.; Umrigar, C. J.; Delley, B.; Lenosky, T. *Phys. Rev. B* **2007**, *75*, 085411.
(14) Gruene, P.; Fielicke, A.; Meijer, G.; Janssens, E.; Ngan, V. T.; Nguyen, M. T.; Lievens, P. *ChemPhysChem* **2008**, *9*, 703.
(15) Jackson, K.; Nellermoe, B. *Chem. Phys. Lett.* **1996**, *254*, 249.

endohedral structures,[16] a number of theoretical and experimental studies have been devoted to the identification of their structures and properties.[17−29] Nevertheless, the influence of different dopants on the structural properties of the host silicon clusters and, in particular, on the growth mechanisms that govern the evolution of all physical and chemical properties is still poorly understood. Up to now, no single experimental method can directly provide detailed information about the geometrical structure of isolated gas-phase clusters. However, in conjunction with theoretical investigations, detailed insight into their structures becomes possible. Photoelectron spectroscopy can clarify the clusters' electronic structures and is mainly used for anionic species,[4,22,27,29,30] while photodissociation experiments point out the stable cluster sizes,[31] and ion mobility measurements[9,10] give information on their collision cross-sections. More direct information on the cluster structure is provided by Raman[6] and infrared[8] spectroscopy. Most recently, it was shown that X-ray absorption spectroscopy can be applied to size-selected cationic clusters, and it has been used to investigate the electronic structure of a number of endohedrally doped Si clusters.[32]

On the theory side, often many energetically close-lying isomers exist for a given cluster, with differences in energy that are within the current error bars of the computations, in particular for density functional theory (DFT) methods (±0.3 eV).[33] Hence, it is clear that theory alone also has difficulties in accurately predicting the global minimum geometry of a cluster. The problem is even more severe for binary clusters due to a much larger amount of possible geometric arrangements. Despite a large number of theoretical efforts in identifying silicon cluster structures, many uncertainties still persist. For example, although a small cluster such as Si_6 has been studied extensively,[34−36] its ground-state geometry has remained a subject of much debate until recently.[37]

IR and Raman spectra reflect the intrinsic structure of a molecular system and contain rich information about its geometry. Recently, Fielicke and co-workers showed that the technique of infrared multiple photon dissociation (IR-MPD) spectroscopy applied to complexes between clusters and rare gas atoms allows the determination of size-specific far-infrared spectra in the gas phase.[14,38−42] The determination of the geometry of the cluster produced in the experiment is obtained upon comparison with theoretically predicted IR spectra. For instance, using such an approach, the structure of Si_8^+ has recently been identified while previous studies missed the true ground state.[42]

In a recent communication,[14] we have reported preliminary results of our combined experimental IR-MPD and theoretical study on the structures of small exohedral silicon clusters doped by V or Cu, Si_nV^+ and Si_nCu^+, for the sizes $n = 6-8$. We have shown that the dopant can simply add to a bare silicon cluster, substitute a Si atom of a bare cluster, or lead to a structural reconstruction producing a new geometry.

The transition metals V and Cu possess distinct electronic configurations, which are expected to lead to different bonding phenomena with silicon clusters, although the transition from exohedral to endohedral doping of Si_n^+ is observed to occur at the same size ($n = 12$) for V and Cu.[43] The Cu atom has filled 3d orbitals and one unpaired electron in the 4s orbital ($[Ar]3d^{10}4s^1$); therefore, Cu has only four orbitals (4s and 4p orbitals) available for the bonding, and its 3d electrons hardly participate. The V atom has three unpaired electrons in 3d orbitals and a filled 4s orbital ($[Ar]3d^3 4s^2$); therefore, it has 9 orbitals (3d, 4s, and 4p orbitals), which can participate in the bonding, which can bear up to a maximum of 9 bonds.

Because Cu has only one unpaired electron and therefore can be treated more conveniently, a large number of theoretical studies have been devoted to Cu-doped silicon clusters.[44−51] Using theoretical methods, Hagelberg's group[44−46] showed for the most stable isomers of Si_nCu, with $n = 4$, 6, 8, and 10, that usually either the Si_n framework is similar to the structure of the ground state or low-lying isomers of the bare Si_n or that Cu is making substitutions in Si_{n+1}. They also demonstrated that the Si−Si interactions largely determine the structure of the Si_n framework in Si_nCu, because the Si−Si interactions are stronger than the Cu−Si interactions.

While there exists much data on vanadium-doped silicon cages, the remarkably stable $V@Si_{16}^+$ cluster being a prominent

(16) Beck, S. M. *J. Chem. Phys.* **1987**, *87*, 4233.
(17) Beck, S. M. *J. Chem. Phys.* **1989**, *90*, 6306.
(18) Hiura, H.; Miyazaki, T.; Kanayama, T. *Phys. Rev. Lett.* **2001**, *86*, 1733.
(19) Khanna, S. N.; Rao, B. K.; Jena, P. *Phys. Rev. Lett.* **2002**, *89*, 016803.
(20) Sen, P.; Mitas, L. *Phys. Rev. B* **2003**, *68*, 155404.
(21) Kumar, V.; Briere, T. M.; Kawazoe, Y. *Phys. Rev. B* **2003**, *68*, 155412.
(22) Ohara, M.; Koyasu, K.; Nakajima, A.; Kaya, K. *Chem. Phys. Lett.* **2003**, *371*, 490.
(23) Neukermans, S.; Wang, X.; Veldeman, N.; Janssens, E.; Silverans, R. E.; Lievens, P. *Int. J. Mass Spectrom.* **2006**, *252*, 145.
(24) Chen, Z.; Neukermans, S.; Wang, X.; Janssens, E.; Zhou, Z.; Silverans, R. E.; King, R. B.; von Ragué Schleyer, P.; Lievens, P. *J. Am. Chem. Soc.* **2006**, *128*, 12829.
(25) Kumar, V. *Comput. Mater. Sci.* **2006**, *36*, 1.
(26) Reveles, J. U.; Khanna, S. N. *Phys. Rev. B* **2006**, *74*, 035435.
(27) Koyasu, K.; Atobe, J.; Akutsu, M.; Mitsui, M.; Nakajima, A. *J. Phys. Chem. A* **2007**, *111*, 42.
(28) Torres, M. B.; Fernández, E. M.; Balbás, L. C. *Phys. Rev. B* **2007**, *75*, 205425.
(29) Grubisic, A.; Wang, H.; Ko, Y. J.; Bowen, K. H. *J. Chem. Phys.* **2008**, *129*, 054302.
(30) Grubisic, A.; Ko, Y. J.; Wang, H.; Bowen, K. H. *J. Am. Chem. Soc.* **2009**, *131*, 10783.
(31) Jaeger, J. B.; Jaeger, T. D.; Duncan, M. A. *J. Phys. Chem. A* **2006**, *110*, 9310.
(32) Lau, J. T.; Hirsch, K.; Klar, Ph.; Langenberg, A.; Lofink, F.; Richter, R.; Rittmann, J.; Vogel, M.; Zamudio-Bayer, V.; Möller, T.; von Issendorff, B. *Phys. Rev. A* **2009**, *79*, 053201.
(33) Ziegler, T.; Li, J. *Can. J. Chem.* **1994**, *72*, 783.
(34) Raghavachari, K. *J. Chem. Phys.* **1986**, *84*, 5672.
(35) Zdetsis, A. D. *Phys. Rev. A* **2001**, *64*, 023202.
(36) Zdetsis, A. D. *J. Chem. Phys.* **2007**, *127*, 014314.
(37) Fielicke, A.; Lyon, J. T.; Haertelt, M.; Meijer, G.; Claes, P.; de Haeck, J.; Lievens, P. *J. Chem. Phys.* **2009**, *131*, 171105.
(38) Fielicke, A.; Kirilyuk, A.; Ratsch, C.; Behler, J.; Scheffler, M.; von Helden, G.; Meijer, G. *Phys. Rev. Lett.* **2004**, *93*, 023401.
(39) Fielicke, A.; von Helden, G.; Meijer, G. *Eur. Phys. J. D* **2005**, *34*, 83.
(40) Fielicke, A.; Ratsch, C.; von Helden, G.; Meijer, G. *J. Chem. Phys.* **2007**, *127*, 234306.
(41) Lin, L.; Höltzl, T.; Gruene, P.; Claes, P.; Meijer, G.; Fielicke, A.; Lievens, P.; Nguyen, M. T. *ChemPhysChem* **2008**, *9*, 17.
(42) Lyon, J. T.; Gruene, P.; Fielicke, A.; Meijer, G.; Janssens, E.; Claes, P.; Lievens, P. *J. Am. Chem. Soc.* **2009**, *131*, 1115.
(43) Janssens, E.; Gruene, P.; Meijer, G.; Wöste, L.; Lievens, P.; Fielicke, A. *Phys. Rev. Lett.* **2007**, *99*, 063401.
(44) Hagelberg, F.; Yanov, I.; Leszczynski, J. *J. Mol. Struct. (THEOCHEM)* **1999**, *487*, 183.
(45) Xiao, C.; Hagelberg, F.; Ovcharenko, I.; Lester, W. A., Jr. *J. Mol. Struct. (THEOCHEM)* **2001**, *549*, 181.
(46) Xiao, C.; Hagelberg, F.; Lester, W. A., Jr. *Phys. Rev. B* **2002**, *66*, 075425.
(47) Hagelberg, F.; Xiao, C.; Lester, W. A., Jr. *Phys. Rev. B* **2003**, *67*, 035426.
(48) Xiao, C.; Abraham, A.; Quinn, R.; Hagelberg, F.; Lester, W. A., Jr. *J. Phys. Chem. A* **2002**, *106*, 11380.
(49) Wu, J.; Hagelberg, F. *J. Phys. Chem. A* **2006**, *110*, 5901.
(50) Oña, O.; Bazterra, V. E.; Caputo, M. C.; Ferraro, M. B.; Fuentealba, P.; Facelli, J. C. *J. Mol. Struct. (THEOCHEM)* **2004**, *681*, 149.
(51) Hossain, D.; Pittman, C. U., Jr.; Gwaltney, S. R. *Chem. Phys. Lett.* **2008**, *451*, 93.

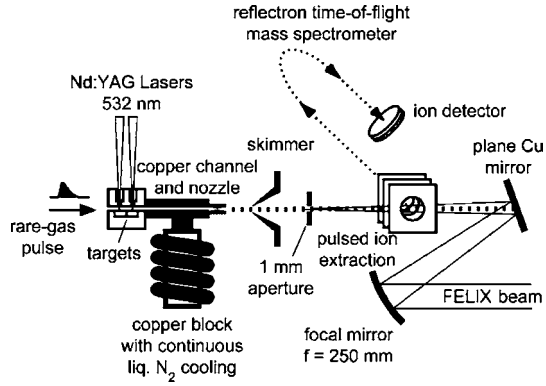

Figure 1. Scheme of the molecular-beam setup for the production of doped silicon cluster−rare-gas complexes and their spectroscopy.

example,[26−28] not much data exists on exohedrally vanadium-doped silicon clusters. Very recently, the photoelectron spectra of anionic $Si_nV_{1,2}^-$ ($n = 3-6$) and a comparison with theory have been reported.[52]

In this article, we report on the results of an extended combined experimental and theoretical study about both series of exohedral-doped silicon clusters Si_nM^+, M = V and Cu, for sizes up to $n = 11$. Experimental spectra are obtained by IR-MPD spectroscopy on the corresponding cluster−argon complexes for cluster sizes of $n = 4-11$ for Si_nV^+ and $n = 6-11$ for Si_nCu^+. Using the combined sets of experimental and calculated spectra, we are able to investigate in detail the growth mechanisms of both series of doped silicon clusters. Most importantly, comparison with the structures of bare silicon clusters allows for an understanding of the effects of the dopants.

2. Experimental Section

The far-infrared spectroscopy experiments on small, doped silicon clusters are performed in a two-stage molecular beam setup, containing a dual laser vaporization source and a time-of-flight mass spectrometer. This setup is connected to a beamline of the Free Electron Laser for Infrared eXperiments (FELIX) at the FOM Institute for Plasma Physics 'Rijnhuizen' in Nieuwegein, The Netherlands, as described elsewhere.[39] The experimental setup is schematically shown in Figure 1.

A transportable pulsed dual-target dual-laser vaporization source, with a repetition rate of 10 Hz,[53] is used for the production of the doped silicon clusters. For this purpose, the second harmonic outputs (532 nm, ∼20 mJ) of two independent Nd:YAG lasers are used to ablate rectangular target plates, which move in a square loop pattern to avoid crater formation. Condensation of the vaporized material takes place in a mixture of mainly helium and argon (∼1%) in the formation chamber. In this process, besides the neutrals, both cationic and anionic clusters are produced. Here, we only investigate the cationic species. The formation chamber is extended by a copper channel, which is cooled using a flow of liquid nitrogen and is thermally isolated from the source body by Teflon spacers. Cluster−rare gas complexes are formed in this cooled reaction channel at a temperature of about 110 K. Following adiabatic expansion into vacuum, the central part of the molecular beam is shaped by a skimmer with a 2 mm diameter opening and a 1 mm aperture, before entering the extraction region of a reflectron time-of-flight mass spectrometer. The mass spectrometer has a resolution of about $M/\Delta M = 800$ around $M = 400$ u. A counter-propagating pulsed far-infrared beam provided by FELIX is focused through the aperture and overlaps with the molecular beam. By adjusting the temporal overlap between cluster beam and laser pulse, we ensure that all clusters detected in the reflectron time-of-flight mass spectrometer have been exposed to the infrared laser light.

The output of FELIX consists of ∼5−8 μs long macropulses with a typical energy of ∼50 mJ. These macropulses are repeated with a rate of 5 Hz. For the spectroscopy of the doped Si clusters, FELIX was tuned over the range from 165 to 625 cm^{-1} (16−60 μm). At the resonant frequencies of the cluster−argon complexes, one or more photons can be absorbed by the cluster. The absorption of photons and subsequent vibrational energy redistribution leads to thermal heating of the cluster and may result in the evaporation of the argon messenger atom. This shows up as a depletion of the ion intensity of the complex in the molecular beam. To take source instabilities into account, the experiments are carried out in toggle mode with the cluster production running at 10 Hz and the FELIX beam at 5 Hz. Using two different channels of a digital storage oscilloscope, alternating mass spectra with and without FELIX irradiation are stored, transferred to the computer, and analyzed. Infrared depletion spectra are recorded by comparing the ion intensities of a given mass after exposure to FELIX with the nonirradiated ion intensities as a function of the FELIX frequency. As time-of-flight mass spectrometry is mass selective, IR spectra of all produced cluster sizes and compositions are obtained simultaneously. From the depletion spectra, IR absorption spectra are calculated as described previously.[39] Such IR-MPD spectra usually closely resemble single photon absorption spectra.[54]

3. Theoretical Methods

DFT is a suitable computational method to treat clusters containing transition metals and for which high-spin states need to be considered. However, none of the available functionals is adequate in giving a consistent description for all properties of all types of clusters. The widely used hybrid B3LYP functional[55−57] was found to yield good results for many systems containing transition metals.[58] In other cases, pure GGA functionals such as BP86[59,60] give better results than B3LYP.[61] In particular, the BP86 functional was found to yield better results than the B3LYP for vibrational frequencies of the transition metal systems when compared with experimental data.[62] On the other hand, B3LYP predicts the atomization energies of small molecules and optical gaps of small silicon quantum dots more accurately.[63,64] Very recently, similar results on relative energies of silicon clusters doped by second row elements were obtained using these two functionals.[65]

The main objective of our work is the assignment of cluster geometries on the basis of IR spectra. The BP86 functional proved to be successful in assigning the IR spectra of bare and transition metal-doped silicon clusters.[14,37,42] Therefore, BP86

(52) Xu, H.-G.; Zhang, Z.-G.; Feng, Y.; Yuan, J.; Zhao, Y.; Zheng, W. *Chem. Phys. Lett.* **2010**, *487*, 204.
(53) Bouwen, W.; Thoen, P.; Vanhoutte, F.; Bouckaert, S.; Despa, F.; Weidele, H.; Silverans, R. E.; Lievens, P. *Rev. Sci. Instrum.* **2000**, *71*, 54.
(54) Oomens, J.; Tielens, A. G. G. M.; Sartakov, B.; von Helden, G.; Meijer, G. *Astrophys. J.* **2003**, *591*, 968.
(55) Lee, C.; Yang, W.; Parr, R. G. *Phys. Rev. B* **1988**, *37*, 785.
(56) Miehlich, B.; Savin, A.; Stoll, H.; Preuss, H. *Chem. Phys. Lett.* **1989**, *157*, 200.
(57) Becke, A. D. *J. Chem. Phys.* **1993**, *98*, 5648.
(58) Ricca, A.; Bauschlicher, C. W., Jr. *J. Chem. Phys.* **1995**, *99*, 9003.
(59) Becke, A. D. *Phys. Rev. A* **1988**, *38*, 3098.
(60) Perdew, J. P. *Phys. Rev. B* **1986**, *33*, 8822.
(61) Jensen, K. P.; Ryde, U. *J. Phys. Chem. A* **2003**, *107*, 7539.
(62) Zhou, M.; Andrews, L.; Bauschlicher, C. W., Jr. *Chem. Rev.* **2001**, *101*, 1931.
(63) Bauschlicher, C. W., Jr. *Chem. Phys. Lett.* **1995**, *246*, 40.
(64) Garoufalis, C. S.; Zdetsis, A. D.; Grimme, S. *Phys. Rev. Lett.* **2001**, *87*, 276402.
(65) Ngan, V. T.; Nguyen, M. T. *J. Phys. Chem. A* **2010**, *114*, 7609.

was used in this work for investigating the geometries and for computing harmonic vibrational frequencies. Figure S2 of the Supporting Information shows the dependence of calculated IR spectra on the chosen functional (BP86 versus B3LYP) for Si_6Cu^+ and Si_7Cu^+. Differences in the vibrational frequencies are typically less than 10 cm^{-1}. Variations in the intensity of the bands, on the other hand, can be quite large.

To evaluate energetic parameters of the clusters, both BP86 and B3LYP functionals are applied using the isomers that are assigned based on the IR spectra as calculated with the BP86 functional. For the B3LYP energetic parameters, the assigned isomers are reoptimized at the B3LYP level. Both functionals are used in conjunction with the all-electron 6-311+G(d) basis sets. The DFT calculations are carried out using the Gaussian03 package.[66]

Initially, the optimizations are performed for a large number of possible geometrical arrangements in different electronic spin states. A search procedure covering as many atomic arrangements as possible is considered. In particular, all the structures available in the literature are taken as initial configurations. In cases of no reported data, such as the Si_nV^+ clusters, initial structures are created by replacing one Si atom by V in the low-lying Si_{n+1} isomers or by capping different sites of Si_n isomers with V. In addition, a large number of initial structures are generated by changing the position of the dopant in a previously located isomer, by adding Si atoms to a smaller doped cluster or by removing Si atoms from a larger one. If an initial shape relaxes to two different structures for two electronic spin states, we take the new structure of the other spin state for further optimizations. Numerous structures are considered; for example, 23 initial structures are generated for Si_4V^+, and 8 low-lying isomers were finally located. As expected, this number increases with cluster size. We found 20 isomers of Si_9V^+ whose energy differences are within 1 eV, while 21 isomers of $Si_{10}V^+$ are located within a relative energy range of only 0.5 eV. Our search procedure does not appear to miss the low-lying isomers as compared to some other search routines. For example, we found new low-lying isomers, which have not been located in a global search using a genetic algorithm[50] as in the cases of Si_4Cu^+ and Si_8Cu^+ (see corresponding sections). In our search procedure the initial optimization is done without symmetry constraints. If the resulting minimum has a specific symmetry, the structure is optimized again with symmetry constraint. Subsequently, harmonic vibrational frequencies are calculated to characterize stationary points and to obtain the infrared spectra.

A low-lying isomer with a soft imaginary frequency is always checked by other methods in the framework of density functional theory, using other functionals such as B3LYP, BLYP, OLYP, and PBE. In the present work, as we study very low-energy vibrational modes, a careful investigation of these modes needs to be done. In the case of nearly symmetrical isomers, reoptimizations with symmetry constraints are carried out to verify if they are really symmetrical or just slightly distorted. Because the computed zero-point energy (ZPE) corrections of the isomeric forms of a specific cluster size are small and almost the same, they are not expected to affect the relative energy ordering. Hence, the relative energies of isomers are obtained from the total electronic energies.

The IR spectra are plotted after folding the stick spectra with a Gaussian line width function of 5 cm^{-1} full width at half-maximum. It is often the case that calculated harmonic vibrational frequencies are slightly shifted from the experimental ones. Therefore, a common practice is to apply a scaling factor to the computed frequencies to bring the predicted spectra in better agreement with the experiment. We thus apply a constant scaling factor of 1.03 to the frequencies calculated at the BP86/6-311+G(d) level for the whole series of clusters considered. This factor is found to give good overall agreement between theoretical predictions and experimental findings for small V- and Cu-doped Si_n^+ clusters,[14] as well as for bare cationic and neutral silicon clusters.[37,42] A scaling factor above 1 could be due to an overestimation of the cluster bond lengths as predicted by the BP86 functional. It has been shown that the errors induced by this functional are rather random;[67] thus, it is conceivable that this scaling factor could be slightly different for different cluster sizes and even for different normal modes of one isomer.

4. Results and Discussion

The following discussion is organized in four parts. The first, section 4.1, focuses on implications of the used methodology, in particular the messenger atom technique. The second, section 4.2, elaborates on the structural determination of the cationic clusters Si_nM^+, M = V, Cu, $n = 2-11$. For the small sizes ($n = 2$, 3 for Si_nV^+ and $n = 2-5$ for Si_nCu^+) no experimental data is available, while a thorough comparison of the theoretical and experimental data is provided for the larger sizes ($n = 4-11$ for Si_nV^+ and $n = 6-11$ for Si_nCu^+). Details of the geometrical and electronic structures will be discussed. In the third, section 4.3, we characterize the different effects that the dopant atoms Cu and V have on the structure of the bare silicon clusters by investigating their growth mechanisms. Finally, in section 4.4, we analyze the thermodynamic stabilities of the exohedrally doped silicon clusters by considering a number of energetic parameters such as average binding energies, secondary difference of energies, fragmentation energy, and frontier orbital HOMO−LUMO gaps.

4.1. Messenger Atom Technique. All experimental IR spectra reported in the subsequent sections are measured using Ar atoms as messenger for the absorption of IR photons by the clusters. Inherent to this messenger atom technique is that not the spectra of the cluster itself but those of the complexes $Si_nM^+ \cdot Ar$ (M = V, Cu) are detected. On the basis of the observation that Ar does not bind to bare silicon clusters, but only to the small transition metal clusters, it has been concluded that Ar attaches to the exohedral transition metal atom and that the interaction between Si and Ar atom is weak.[43] Further, the Ar binding energy to the cationic V-doped clusters amounts to about 0.15 eV only.[43] Hence, it is assumed that the Ar acts as a true messenger not influencing the structures and IR spectra of the clusters significantly. To verify these assumptions, the geometries and IR spectra of the low-lying isomers of Si_6V^+ and Si_6Cu^+ have been compared with the geometries and IR spectra of the corresponding Ar complexes. Indeed, the Ar atom binds strongest to the transition metal dopant atom and the Ar−V and Ar−Cu distances are around 2.5−2.7 Å whereas the Ar−Si distances are larger than 5 Å. The comparison of the IR spectra of the Ar-free clusters and the corresponding Ar−cluster complexes is illustrated in the Supporting Information. The deviations between the IR spectra of clusters with and without Ar are not significant; some frequencies are subjected to a very

(66) Frisch, M. J.; et al. *Gaussian 03, Revision C.02*; Gaussian, Inc.: Wallingford, CT, 2004.

(67) Jensen, K. P.; Roos, B. O.; Ryde, U. *J. Chem. Phys.* **2007**, *126*, 014103.

small blue shift (less than 5 cm^{-1}) upon Ar attachment. For most isomers, the intensities of a few peaks tend to increase as the Ar atom is attached, and this leads to changes in the relative intensities of bands. The energy ordering of the various isomers with Ar remains identical to that of the Ar-free isomers. Because of the very weak effect of the Ar messenger, unless otherwise noted, we hereafter only consider the Ar-free clusters.

In the case exohedral and endohedral metal-doped isomers coexist in the cluster beam, the messenger technique will be biased toward the exohedral isomer because of the selective Ar attachment. The abundance of structures without metal-exposure, however, is expected to be small because the fraction of clusters that form Ar complexes is large in our experiment (between 60% and 100% except for $Si_{11}V^+$; see ref 43). The lower fraction of Ar complexes for $Si_{11}V^+$ is discussed in section 4.2. Such bias of the messenger technique toward certain isomers was observed recently:[68] the planar Au_{12}^- isomer attaches Ar much more efficiently than a coexisting 3D isomer.

4.2. Structural Determination and Vibrational Spectroscopy. We present the results size by size, with increasing cluster size. The Si_nM^+ clusters with the same number of Si atoms are successively presented. The isomers considered for each cluster size are invariably labeled as **iso1**, **iso2**, **iso3**, etc., with increasing relative energy. Their structures are shown and labeled in the corresponding figures accordingly. Geometrical parameters of the bare and doped silicon clusters used for discussion are computed at the BP86/6-311+G(d) level in this section.

4.2.1. Si_2M^+. The most stable structures of both Si_2V^+ and Si_2Cu^+ cations are isosceles triangles having $^3B_1$ ground states. The triangular forms for the singlet and quintet states undergo a geometrical relaxation while keeping a C_{2v} symmetry but are associated with higher energies (1.07 and 0.52 eV for Si_2V^+; 0.60 and 2.26 eV for Si_2Cu^+, respectively).

All three vibrational normal modes of the ground state of either Si_2V^+ or Si_2Cu^+ are infrared active. The energetically highest vibrations are the symmetric Si−Si stretches, and these have almost the same frequencies (465 cm^{-1} for Si_2Cu^+ and 473 cm^{-1} for Si_2V^+), which are comparable to the stretching frequency of the triplet diatomic Si_2 (479 cm^{-1} at the same level of theory). This similarity can be attributed to their nearly equal Si−Si bond strengths.

4.2.2. Si_3M^+. While for Si_3Cu^+, we find a C_{2v} planar rhombus in the singlet $^1A_1$ electronic state as the lowest-energy structure, for Si_3V^+ a C_{3v} pyramidal structure in a triplet $^3A_1$ state is favored (more isomers are displayed in the Supporting Information). For both, the positive charge is mainly distributed over the Si_3 framework. Hence, the pyramid of Si_3V^+ is built up by adding the V atom to the Si_3^+ triangle.[10,12] In contrast, the planar ground-state structure of Si_3Cu^+ is constructed by replacing one Si by Cu at one apex of the shorter diagonal of the rhombus Si_4^+.[10,12]

4.2.3. Si_4V^+. Figure 2a shows the structures of the four lowest-lying isomers **iso1**−**iso4** of Si_4V^+, identified in our calculations, and their IR spectra, which are compared with the experimental IR-MPD spectrum of Si_4V^+·Ar. This cluster is experimentally characterized by one peak centered at 414 cm^{-1} and an additional absorption around 200 cm^{-1}. These two features are reproduced by the most stable isomer **iso1** having a singlet ground state, which is a C_{3v} trigonal bipyramid with the V atom occupying an axial position. In the calculated spectrum, the intense peak centered at 411 cm^{-1} is characterized as an A_1 mode and describes a stretching vibration of the tetrahedral Si_4 moiety. The peak at 169 cm^{-1} is due to an E mode, which is going to split up into two energetically close modes upon symmetry lowering when an Ar atom is attached to the cluster. The A_1 mode fits the experimental band nicely, and the E mode, which appears very sensitive to the method and basis set employed, can be assigned to the experimental absorption band around 200 cm^{-1}. The calculated IR spectra of the higher-energy isomers **iso2**, **iso3**, and **iso4** do not match the experimental results.

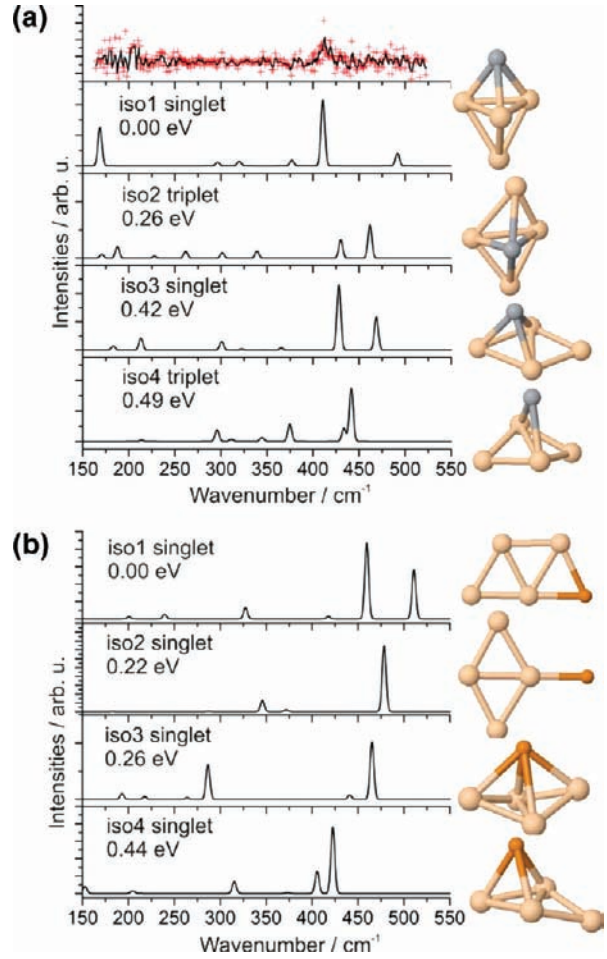

Figure 2. (a) The upmost panel shows the experimental IR-MPD spectrum of Si_4V^+·Ar. Lower panels show the calculated IR spectra for the four low-lying isomers of Si_4V^+. (b) The calculated IR spectra for the four low-lying isomers of Si_4Cu^+.

In comparison to the bare silicon clusters, the lowest-lying isomer **iso1** can be described as a substitution of a Si atom by V at an axial position of the C_{2v} trigonal bipyramid Si_5^+.[10,12] Following substitution, the three Si atoms at equatorial positions come significantly closer to each other (the distances being 2.454 Å in Si_4V^+ as compared to 2.940 or 3.212 Å in Si_5^+) while the two Si atoms in equatorial and axial positions are moving away (distances being 2.510 Å in Si_4V^+ as compared to 2.271 or 2.396 Å in Si_5^+). Substituting an equatorial Si of the trigonal bipyramid Si_5^+ by V leads to **iso4** that is 0.49 eV higher in energy relative to the lowest-energy isomer **iso1**. Adding V onto the rhombus Si_4 leads to higher-energy isomers **iso2** and **iso3.**

4.2.4. Si_4Cu^+. Our search procedure locates two new low-lying isomers **iso2** and **iso4** (Figure 2b), which have not been found previously, not even in a global search using a genetic

(68) Huang, W.; Wang, L. S. *Phys. Rev. Lett.* **2009**, *102*, 153401.

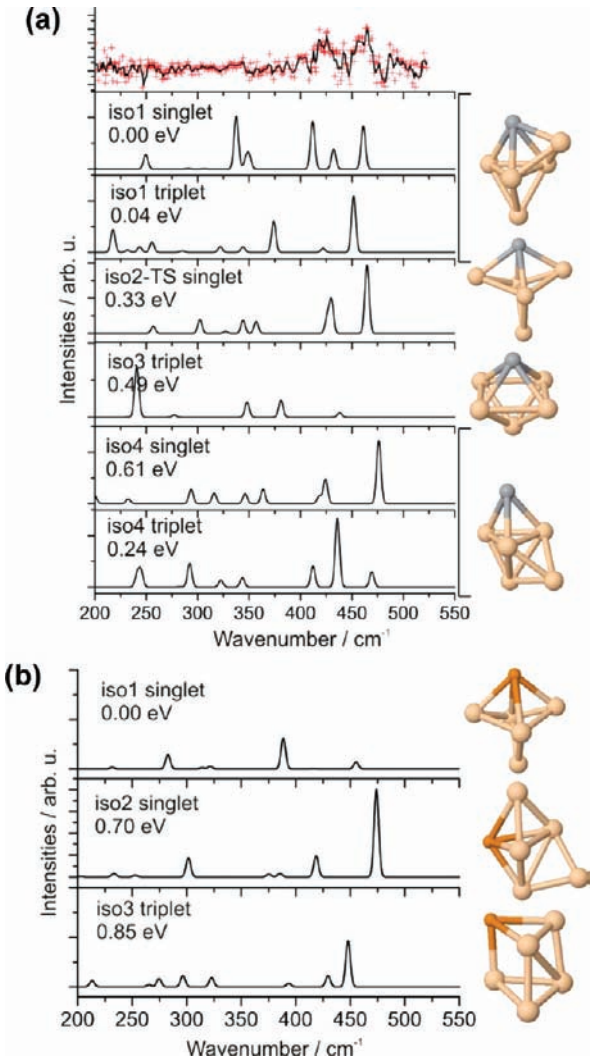

Figure 3. (a) The upmost panel shows the experimental IR-MPD spectrum of $Si_5V^+ \cdot Ar$. Lower panels show the calculated IR spectra for the five low-lying minima and one transition structure **iso2-TS** of Si_5V^+. (b) The calculated IR spectra for the three low-lying minima of Si_5Cu^+.

algorithm.[50] The electronic singlet ground state **iso1** is in agreement with the result of Xiao et al.[46] It is still planar and built up by adding Cu to an edge of the rhombus Si_4^+.[10,12] Unlike Si_4V^+, the trigonal bipyramid turns out to be a high-energy isomer for Si_4Cu^+ (1.89 eV higher than the ground state and not shown in Figure 2b). The computed IR spectrum of the most stable isomer **iso1** contains two intense peaks located at 459 and 510 cm^{-1}, which correspond to the in-plane stretching of Si−Si bonds and the linear Si−Si−Cu moiety vibration, respectively. Unfortunately, we could not record the experimental IR spectrum for this cluster.

4.2.5. Si_5V^+. Figure 3a illustrates the results for Si_5V^+ including the calculated IR spectra for four isomers **iso1**−**iso4.** These structures are all related to the three O_h, C_{2v}, and C_s structures previously discussed as contributing to the fluxional ground state of Si_6.[36] The most stable isomer of Si_5V^+ turns out to be the low symmetry C_s **iso1** having a low-spin state $^1A'$. However, the triplet $^3A''$ state is almost degenerate with the singlet, characterized by a marginal adiabatic singlet−triplet gap of 0.04 eV favoring the low spin state. The C_{2v} **iso2** that is a transition structure (TS) possessing an imaginary B_2 mode of 114*i* cm^{-1} lies 0.33 eV above the ground state. The calculations performed by other functionals also predict the **iso2** as TS with comparable energy differences of around 0.3 eV. Relaxing the geometry of **iso2-TS** along the imaginary mode leads to the most stable isomer **iso1**. Not surprisingly, the motions of the fundamental vibrational modes for **iso1** and **iso2-TS** have similar frequencies but differ in intensity. Both calculated spectra are in good agreement with the experiment in the range of 400−475 cm^{-1}. The band at 430 cm^{-1} of **iso2-TS** includes two vibrational modes, which are separated in **iso1**. However, the pronounced band at 338 cm^{-1} of **iso1** becomes a low-intensity band in **iso2-TS** and is not found in the experimental counterpart. Given the limited quality of the experimental spectrum (related to the small fraction of Ar complexes that are formed for Si_5V^+ in the molecular beam), no definite assignment of the Si_5V^+ geometry can be made.

4.2.6. Si_5Cu^+. Three low-lying structures **iso1**−**iso3** and their calculated IR spectra are shown in Figure 3b. An experimental IR spectrum could, however, not be measured for Si_5Cu^+. The singlet state of the C_s structure **iso1** ($^1A'$), which is obtained by relaxing a tetragonal bipyramid with the Cu atom situated at an axial position, is the lowest-lying isomer of Si_5Cu^+. However, a similar structure with C_{2v} symmetry is found to possess a very soft imaginary frequency (<20*i* cm^{-1}), which can also be found by the BLYP and B3LYP functionals but are not confirmed by the OLYP and PBE functionals. The energy difference between both geometries is only 0.001 eV. Incorporation of zero-point energies leads to a basically flat potential energy surface. The imaginary mode in the C_{2v} form describes the movement of Cu back and forth relative to the symmetric plane, meaning that, in this case, Cu plays the role of the fluxional atom instead of Si in Si_6.[36]

4.2.7. Si_6V^+. Although the identification of this cluster has been reported in our previous communication,[14] we continue here with a deeper discussion. Experimentally, Si_6V^+ is characterized by an intense band at 398 cm^{-1}, which is compared with the calculated IR spectra of four low-lying isomers (Figure 4a). The face-capped tetragonal bipyramid **iso1** ($^1A'$) and the pentagonal bipyramid **iso2** ($^3A_2$) are of comparable energy and are therefore competitive for the ground state. However, **iso1** can easily be excluded by comparing with the experiment because it has a combined Si−Si stretching vibration leading to the pronounced peak at 474 cm^{-1}, which is at a much higher frequency than the experimental band at 398 cm^{-1}. In addition, its spectrum contains several other bands which are not seen in the experiment. The triplet pentagonal bipyramid **iso2** with an equatorial V atom exhibits the most intense peak at 394 cm^{-1}, much closer to the observed band. This isomer has an additional weak peak at 434 cm^{-1} due to a couple of A_1 and B_2 modes corresponding to the in-plane movement of atoms in the pentagon and parallel-to-plane movement of the two Si atoms on top. Among the four lowest-lying isomers only isomer **iso2**, which fits the experiment best, is formed by substitution of Si by a V atom. **iso3** and **iso4** are adsorptive structures, and **iso1** is built up by a reconstruction.

4.2.8. Si_6Cu^+. The experimental spectrum of this cluster looks similar to that of Si_6V^+, but the observed band is at higher frequency (~445 cm^{-1}) and broader. Figure 4b compares the experimental and calculated IR spectra of some low-lying states. The identified lowest-energy isomer of Si_6Cu^+ is the singlet **iso1**, a bicapped trigonal bipyramid, whose calculated IR spectrum reproduces the experimental data best. Initially, the distorted **iso1** form was located as a true minimum. Then a C_s form was optimized under a symmetry constraint. But the C_s

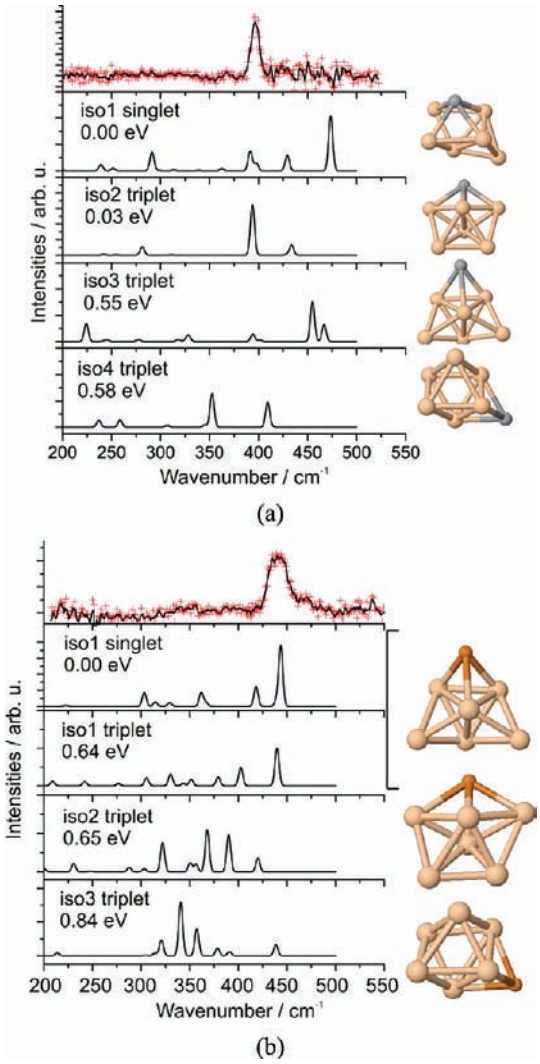

Figure 4. The upmost panel shows the experimental IR-MPD spectrum of $Si_6M^+ \cdot Ar$. Lower panels show the calculated IR spectra for some low-lying minima of Si_6M^+. (a) M = V; (b) M = Cu.

form is 0.004 eV less stable than the nonsymmetric isomer and possesses a small imaginary frequency (44*i* cm^{-1}). The imaginary frequency is also found for the C_s geometry by the B3LYP and BLYP functionals, while the C_s geometry is a local minimum when using the OLYP and PBE functionals. For the ease of vibrational analysis, the C_s form of **iso1** is used to explain the IR spectrum of Si_6Cu^+, which includes one intense absorption at 444 cm^{-1} (A″ mode), a less intense peak at 418 cm^{-1} (A′ mode) and a very low-intensity peak at 439 cm^{-1} (A′ mode). Each of the three normal modes represents a combined Si−Si stretching vibration, whereas the Cu atom hardly moves. The broad experimental band likely arises from a combination of the three close-energy absorptions.

A triplet state of **iso1** lies 0.64 eV higher than the singlet ground state. The triplet IR spectrum looks similar to that of the singlet, but the large energy difference makes a contribution of the triplet state rather unlikely. Previously, Xiao et al.[46] reported a distorted form of the **iso1** singlet state as the lowest-energy isomer, but the other forms considered here were not identified for Si_6Cu^+. **iso1** and **iso3** correspond to face adsorptions of Cu on the Si_6-C_s and Si_6-D_{4h} structures, respectively, while **iso2** is a substitution of Si by Cu at an equatorial position in the pentagonal bipyramid ground state of Si_7^+.[42]

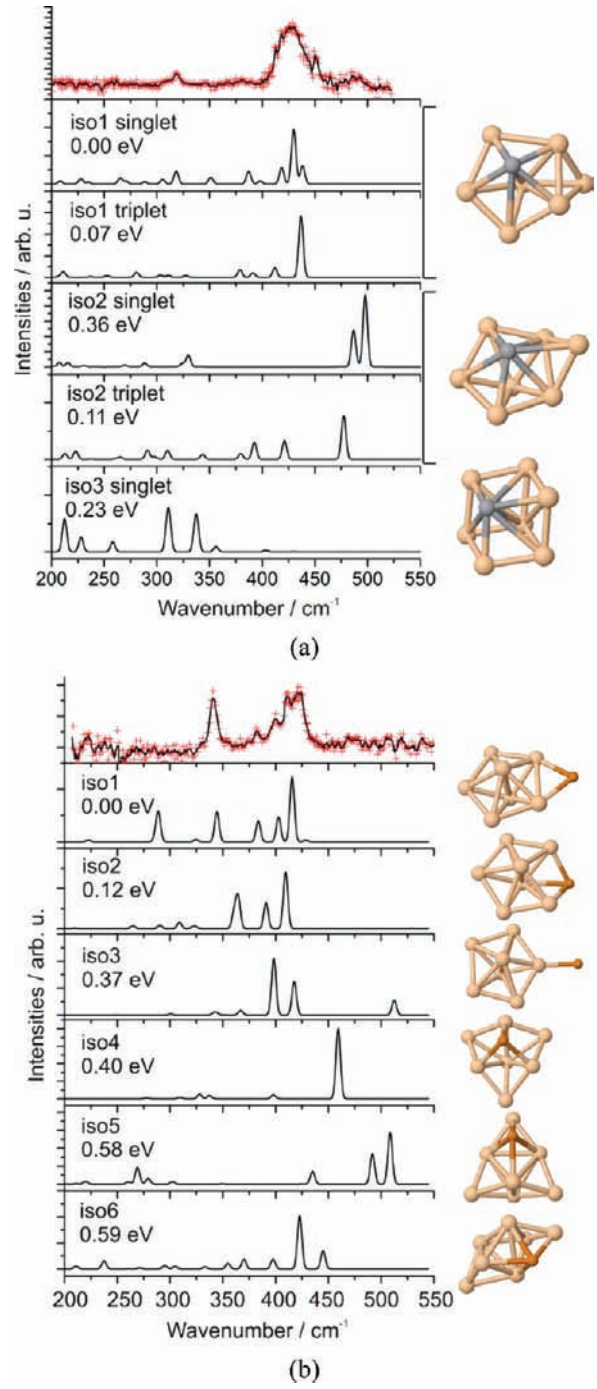

Figure 5. The upmost panel shows the experimental IR-MPD spectrum of $Si_7M^+ \cdot Ar$. Lower panels show the calculated IR spectra for some low-lying minima of Si_7M^+. (a) M = V; (b) M = Cu.

4.2.9. Si_7V^+. The experimental and computed IR spectra for five low-lying states are compared in Figure 5a (more isomers are shown in the Supporting Information). The two energetically lowest isomers, namely **iso1** and **iso2**, can be derived by substituting V into an axial position of an edge-capped pentagonal bipyramid of the Si_8^+ cation[42] that after relaxation turn into a face-capped pentagonal bipyramid. **iso3** is obtained by replacing one Si by V in the bicapped octahedral ground-state structure of the neutral Si_8.[10,12]

Experimentally, we observe a very broad band centered at 425 cm^{-1} and additional low-intensity bands around 317 and 470 cm^{-1}. By comparing the IR spectra, the singlet state of

iso1 appears to be present in the molecular beam, as it exhibits an intense peak centered at 430 cm^{-1} and two less intense peaks at 418 and 438 cm^{-1}. The three absorptions can be assigned to the broad band at 425 cm^{-1}. This isomer also exhibits a band at 317 cm^{-1} as experimentally observed. However, it has no modes that could explain the absorption band around 470 cm^{-1}. A triplet state of **iso1**, which is only 0.07 eV higher in energy, cannot be excluded based on the experimental spectrum as its sharp peak at 437 cm^{-1} lays within the broad experimental band. Although these two states adopt similar shape, their atomic distances are rather different, and therefore their fundamental vibrational motions are not the same. For example, both of them have a band at ~438 cm^{-1}; however, this represents a combination of two V−Si bond stretch vibrations in the singlet state, while in the triplet state it describes the combined motions of two Si−Si bonds.

The triplet state of **iso2**, being 0.11 eV above the lowest-energy state, bears an intense absorption at 477 cm^{-1}, which is close to the experimental low-intensity signal at 470 cm^{-1} and some less intense ones lying within the observed broad band. The calculated frequency of 477 cm^{-1} represents stretching motions of three Si atoms of a rhombic moiety. We argue for the presence of the triplet **iso2** in the molecular beam, and its small contribution to the observed IR spectrum. In summary, the spectra of three closely lying states, whose structures are formed by axial substitutions of a Si atom by a V atom in Si_8^+, can be responsible for the experimental spectrum of Si_7V^+. Whereas singlet states of **iso1** and **iso2** seem essential to explain all experimental absorption bands, the contribution of the triplet state of **iso1** cannot be excluded either.

4.2.10. Si_7Cu^+. For the larger Si_nCu^+ ($n \geq 7$) clusters, the singlet states are consistently lower in energy than the corresponding triplet states (>1 eV). Therefore, we discuss hereafter only the electronic singlet states of the isomeric forms. Likewise this is the case for the larger V-doped Si cluster cations ($n > 7$, except $n = 10$). Figure 5b displays six low-lying singlet isomers of Si_7Cu^+ and their calculated IR spectra in comparison with the experimental spectrum. The three lowest-lying isomers contain a pentagonal bipyramidal Si_7 unit, which also forms a building block of small cationic Si_n^+ clusters, $n = 7-9$.[42] The Cu atom binds to an equatorial edge, a face, or an equatorial apex of the pentagonal bipyramid giving rise to **iso1** (C_{2v}), **iso2** (C_s), and **iso3** (C_{2v}), respectively. Because they all retain a pentagonal bipyramid building block, they have some common vibrational modes corresponding to the movements of the Si_7 framework.

Interestingly, **iso1** is also a low-coordinated substitutive derivative of the edge-capped pentagonal bipyramid Si_8^+,[42] in which Cu takes the position of the capping Si atom. The calculated IR spectrum of **iso1** nicely reproduces the four experimental bands in the range of 380−420 cm^{-1} (calculated: 384 cm^{-1}, A_1; 403 cm^{-1}, A_1; 416 cm^{-1}, B_2; and 429 cm^{-1}, A_1) and the sharp peak at 340 cm^{-1} (calculated: 344 cm^{-1}, B_2). These fundamental vibrations are delocalized deformations of the Si framework; therefore, the resulting frequencies are rather low as compared to more localized Si−Si stretches. The computed bands of **iso1** around 290 cm^{-1} relate to B_2 and A_1 modes but are not observed in the experimental depletion spectrum of $Si_7Cu^+ \cdot Ar$. Nevertheless, on the mass of Si_7Cu^+ we find a weak but significant signal increase at 302 cm^{-1}, which indicates its formation out of a dissociating complex. The absence of this band in the depletion spectrum of $Si_7Cu^+ \cdot Ar$ may be attributed to a distortion of the spectrum due to fragmentation of even larger Ar complexes, although the mass spectrum does not show abundant complexes of Si_7Cu^+ with more Ar atoms. In all other parts of the IR spectrum the growth for Si_7Cu^+ mirrors the depletion of $Si_7Cu^+ \cdot Ar$. We therefore suggest **iso1** to be the experimentally detected isomer. As a matter of fact, the motion of the calculated band at 290 cm^{-1} is related to two Si−Cu bonds, and the binding of an Ar atom to the Cu atom may affect the IR intensity of this mode. The Cu-edge-capped pentagonal bipyramid structure **iso1** is also consistent with the available photodissociation data,[31] which found that $Si_7^+ + Cu$ is the primary dissociation channel of Si_7Cu^+.

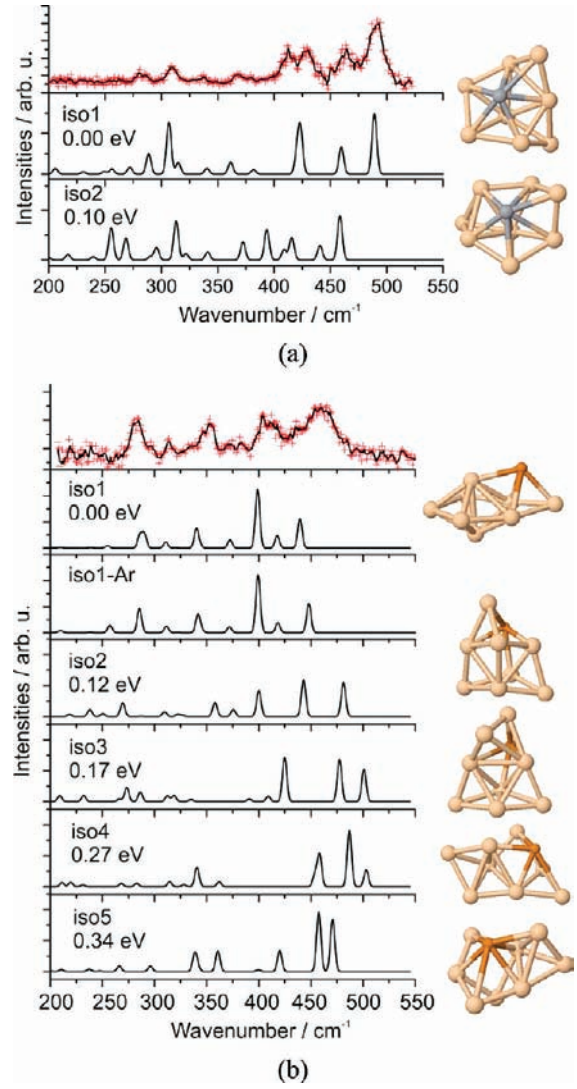

Figure 6. The upmost panel shows the experimental IR-MPD spectrum of $Si_8M^+ \cdot Ar$. Lower panels show the calculated IR spectra for some low-lying minima of Si_8M^+. (a) M = V; (b) M = Cu.

The less stable isomer **iso3** exhibits an A_1 mode located at 512 cm^{-1}, which is the highest vibrational frequency for the three lowest-lying isomers. This mode corresponds to a stretching of the Si−Cu bond. Because the experimental spectrum does not show any band at that high frequency, the possibility of a monocoordinated Cu center can be excluded. The isomers **iso4**, **iso5**, and **iso6** are significantly higher in energy and their IR spectra do not fit the experiment.

4.2.11. Si_8V^+. A comparison between the theoretical and experimental IR spectra of this cation is fully reported in our earlier Communication.[14] Thus, in Figure 6a we only present

the two lowest-lying isomers, which are interesting to compare, as they are structurally very similar (a larger set of 15 isomers is displayed in the Supporting Information). The IR-MPD spectrum of the $Si_8V^+ \cdot Ar$ complex is characterized by two bands centered at 466 and 493 cm^{-1}, a doublet at 414 and 433 cm^{-1}, and also some less intense bands between 275 and 375 cm^{-1}. Despite the existence of no less than six isomers whose relative energies range within only 0.2 eV, the most stable isomer **iso1** is assigned to be the one produced in the experiment. Indeed, **iso1** features two peaks situated at 460 and 489 cm^{-1}, and two additional normal modes at 421 and 424 cm^{-1} that, in contrast to the experiment, are not resolved and appear as a single band in the simulation. In the low-frequency region, this isomer also contains two intense absorptions at 289 and 307 cm^{-1}. Concerning the shape, **iso1** is a bicapped pentagonal bipyramid in which the V atom substitutes Si in an axial position. **iso2** has a very similar structure as **iso1** and is just 0.1 eV higher in energy. The structural difference between them is that one Si atom is moving to an adjacent Si−Si−Si face. However, comparing the IR spectra, **iso2** can be ruled out as an appropriate candidate because its highest predicted vibration at ∼458 cm^{-1} is relatively low with respect to the highest experimental band at 493 cm^{-1}. In contrast, **iso1** has a band at 489 cm^{-1}, which describes the stretching of the nearly linear Si−Si−Si moiety (∠SiSiSi = 169°) consisting of an equatorial and the two capping Si atoms.

4.2.12. Si_8Cu^+. The experimental spectrum of Si_8Cu^+ includes a very broad band centered at 460 cm^{-1} and four lower-frequency signals at 281, 312, 353, and 405 cm^{-1} (Figure 6b). A structure previously reported[46] as the ground state of this cation turns out to be the third lowest-energy isomer **iso3** that is 0.17 eV above the lowest-lying minimum **iso1** found in the present work. Apparently, **iso3** is not abundant in the experiment, as it has intense bands at significantly higher frequencies than the experimental ones.

The ground state **iso1** is a C_s bicapped pentagonal pyramid ($^1A'$ electronic state) in which Cu bridges one apex of the pentagonal bipyramid and the capping Si atom. Even though this cluster has been studied widely including a genetic algorithm search,[50] this ground-state structure has never been located. Its computed IR spectrum presents a good agreement with the experiment. The only difference between experiment and calculated spectra of **iso1** is that the experimental band centered at 460 cm^{-1} is broader and blue-shifted compared to the computed one at 439 cm^{-1}. However, this can be rationalized by taking the Ar-messenger atom into account. The motion of the highest-energy absorption is a combination of stretching of the Si1−Si2 and Si1−Si3 bonds (Si1 is the Si atom capping on the edge Si2−Si3 of the pentagonal bipyramid). Because these three Si atoms are directly bound to Cu, an attachment of Ar to Cu reduces these bond distances from 2.450 to 2.434 Å, while other bonds remain unchanged or marginally increase. A small decrease in bond length induces a significant blue shift in vibrational frequency of this normal mode from 439 to 448 cm^{-1}, whereas changes for the other modes are within only 2 cm^{-1}. Hence, the attachment of Ar brings the calculated position of the highest energy band closer to the observed frequency. In addition, small differences in the cluster−argon bond will result in different frequencies for this particular band (as only the frequency of this band shifts significantly upon Ar attachment), which can be a reason for its broadening.

The existence of **iso2** in the molecular beam might also be considered, because its spectrum has some features similar to those of the experiment. However, the highest-energy band of this isomer is centered at 481 cm^{-1}, and upon adding an Ar atom, it increases to 490 cm^{-1}, which is much higher than the observed value of 460 cm^{-1}. In contrast to **iso1**, addition of Ar moves this band away from the experimental value. In summary, the C_s bicapped pentagonal pyramid **iso1**, which is located for the first time in our work,[14] is assigned as the Si_8Cu^+ ground-state structure.

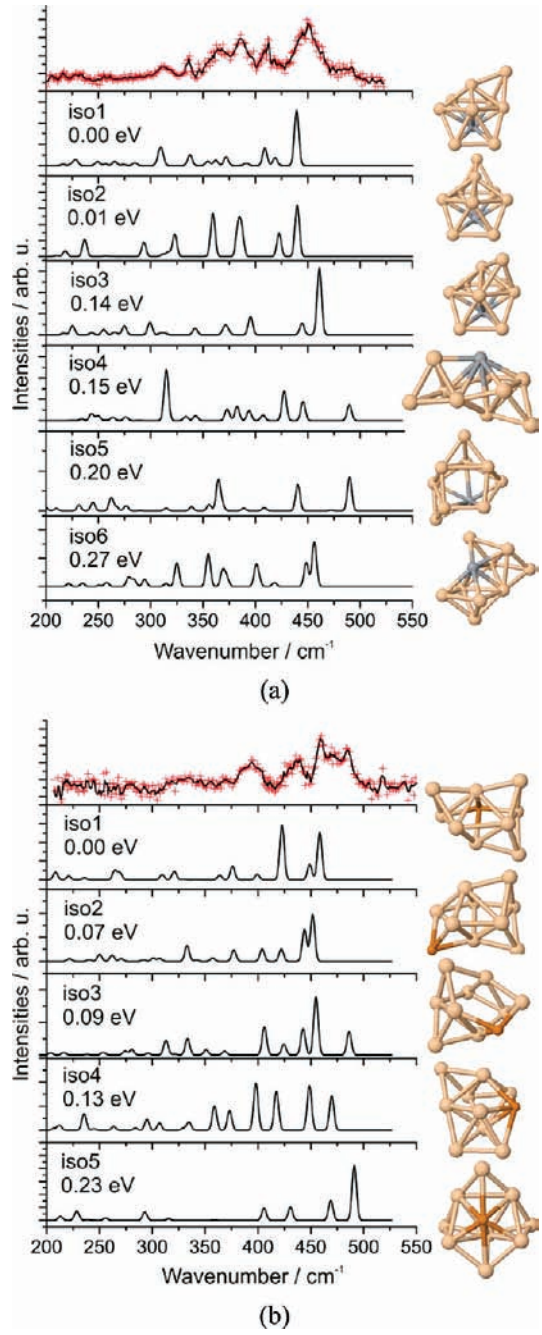

Figure 7. The upmost panel shows the experimental IR-MPD spectrum of $Si_9M^+ \cdot Ar$. Lower panels show the calculated IR spectra for some low-lying minima of Si_9M^+. (a) M = V; (b) M = Cu.

4.2.13. Si_9V^+. In the experimental IR spectrum shown in Figure 7a, Si_9V^+ exhibits one band centered at 450 cm^{-1}, one less intense peak at 410 cm^{-1}, and a doublet at 365 and 387 cm^{-1}. In addition, some low-intensity signals in the range of 300−350 cm^{-1} need to be taken into account as well. The six lowest-lying isomers in the electronic singlet state and their IR

spectra are presented in Figure 7a (more isomers are displayed in the Supporting Information). The most stable isomer **iso1**, which is formed by capping Si_8V^+ with one additional Si atom, can account for most vibrational features in the experimental spectrum. The IR spectrum of **iso2**, with a structure similar to and only 0.01 eV less stable than **iso1**, also matches well with the experiment even considering the relative intensities, especially for the experimental doublet at 365 and 387 cm^{-1}. In addition, another tricapped pentagonal bipyramid **iso3**, which is 0.14 eV above **iso1**, cannot be excluded because its pronounced peak at 460 cm^{-1} is in the range of the experimental highest-energy band (425−475 cm^{-1}).

The three lowest-energy isomers, which all have a Si_8V base that is a portion of a Si_{12} icosahedron with V in the center and with two Si vertices of degree 5, all can explain the experimental spectrum. No definitive assignment can be made for the structure of Si_9V^+, though based on the relative intensities of the absorption bands, **iso2**, which is only 0.01 eV above **iso1**, is the best candidate.

4.2.14. Si_9Cu^+. Five low-lying isomers of Si_9Cu^+, which are all based on a pentagonal bipyramidal shape, are calculated to be very close in energy (Figure 7b). **iso1**, **iso2**, and **iso3** retain the bicapped pentagonal bipyramidal ground state structure of Si_9^+ (ref 42) but are strongly distorted in different ways compared to the cationic bare cluster. Cu replaces an equatorial Si atom of the pentagonal bipyramidal frame giving **iso1,** while it adsorbs to different faces yielding the other structures. **iso4** has a shape similar to the lowest-lying isomer of Si_9V^+. **iso5** is a substitutive derivative of a tricapped bipyramidal pentagon, a higher-energy isomer of Si_{10}^+ (identified in this work and lying 0.47 eV higher than the tricapped trigonal prism global minimum[42]). We find that **iso3** is 0.09 eV above the lowest-lying isomer and appears to provide the best fit with the experimental measurement. The four intense peaks at 406, 443, 455, and 486 cm^{-1} of the calculated spectrum of **iso3** can be assigned to the experimental bands centered at 393, 437, 458, and 483 cm^{-1}. Similar to some other clusters, the highest frequency band originates from a stretching of a nearly linear Si−Si−Si moiety. Two peaks in the middle, at 443 and 455 cm^{-1}, correspond to symmetric stretching vibrations of the two rhombuses composed of Si atoms. Both **iso1** and **iso2** miss a band corresponding to the absorption at 483 cm^{-1}. The quality of the experimental spectrum, though, does not allow definitively ruling them out.

iso3 contains a distorted trigonal prism which is a part of the tetra-capped trigonal prism ground-state structure of Si_{10}^+.[42] As both structural features emerge in low-energy isomers, this suggests that structures of Cu-doped silicon clusters tend to change from a pentagonal bipyramid type to a trigonal prism type at this size (nine Si atoms).

4.2.15. $Si_{10}V^+$. For the larger clusters, the identification is getting much more difficult due to the quality of the experimental spectra and the emergence of many possible isomeric forms. Twenty-one isomers of $Si_{10}V^+$, illustrated in the Supporting Information, are located within a relative energy range of 0.5 eV. In Figure 8a, we show the ten lowest-lying identified states and their calculated IR spectra in comparison with experiment. Many isomers retain the pentagonal bipyramid building block with V situated at one top. However, the computed lowest-energy structure has a trigonal prism unit, and its calculated IR spectrum is in the range of the observed band. Both singlet and triplet states of the isomer **iso2** have quite strong signals below 400 cm^{-1}, which are not detected in the

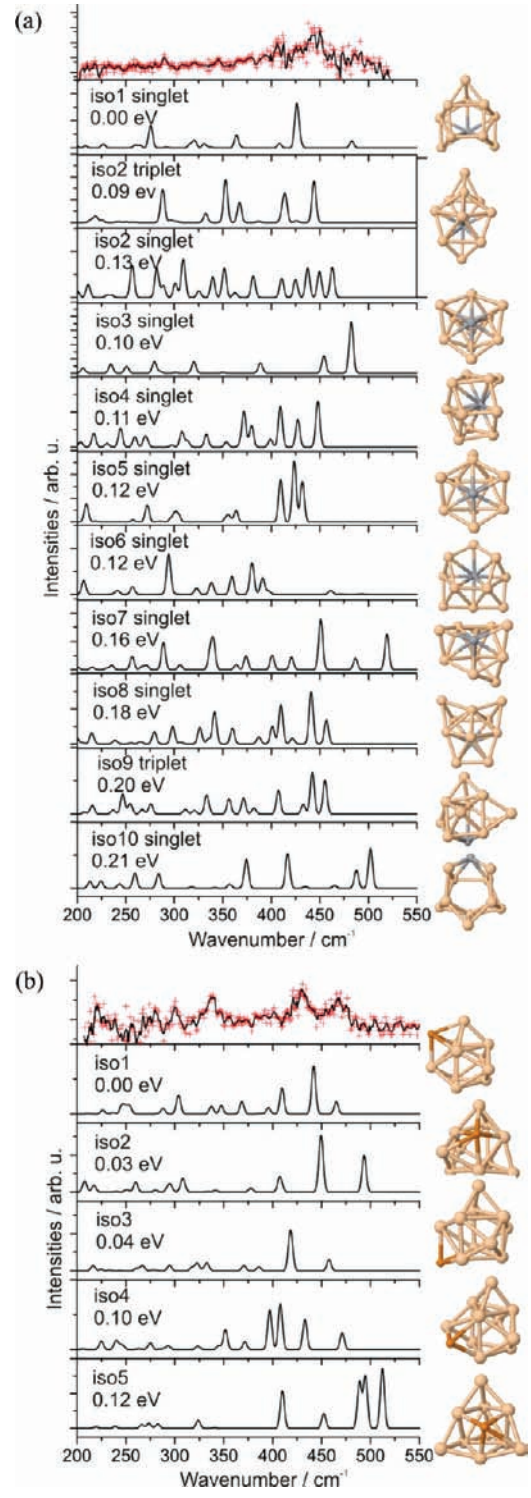

Figure 8. The upmost panel shows the experimental IR-MPD spectrum of $Si_{10}M^+ \cdot Ar$. Lower panels show the calculated IR spectra for some low-lying minima of $Si_{10}M^+$. (a) M = V; (b) M = Cu.

experiment. Among many close-lying isomers, **iso5** and **iso8**, which lie 0.12 and 0.18 eV above the energetically lowest isomer, respectively, seem to give a better match with the experimental spectrum. The theoretical results indicate a coexistence of pentagonal bipyramid and trigonal prism isomers for $Si_{10}V^+$ while this is observed at a smaller size, Si_9Cu^+, for Cu-doped species.

4.2.16. $Si_{10}Cu^+$. Figure 8b shows IR spectra and structures for $Si_{10}Cu^+$ (more isomers are displayed in the Supporting

Information). The experimental spectrum is reasonably well reproduced by the calculated one for **iso1**. Its structure is a pentacapped trigonal prism in which Cu is added to one edge of the tetracapped trigonal prism that has recently been confirmed by experiment for the bare Si_{10}^+ cluster.[42] Three isomers, namely **iso2**, **iso3**, and **iso4**, have previously been reported as the energetically lowest-lying ones by Xiao et al.[46] The energetically lower structure **iso1** has not been found by these authors. **iso3** (+0.04 eV) may also contribute to the experimental spectrum, while the presence of the isoenergetic **iso2** (+0.03 eV) can be excluded as it exhibits a band at high frequency, which is not observed in the experiment. By comparison of the computed and observed IR spectra, we would suggest the adsorptive derivatives **iso1** to be responsible for the experimental IR spectrum of $Si_{10}Cu^+$, but the existence of **iso3** cannot be excluded on the basis of the current experimental result.

4.2.17. $Si_{11}V^+$. Figure 9a illustrates the IR spectra and structures of $Si_{11}V^+$ (more isomers are shown in the Supporting Information). Because the recorded spectrum of $Si_{11}V^+$ has a low signal-to-noise ratio, it is difficult to identify the structure of this cluster. The experimental spectrum has some bands in the range of 340−460 cm^{-1} and two sharp peaks centered at 200 and 493 cm^{-1}.

At least a fraction of $Si_{11}V^+$ is observed to bind Ar, and therefore it has been concluded previously that such clusters are exohedrally doped.[43] This excludes the possibility to have only V encapsulated by silicon cages, such as the lowest-energy isomer **iso1**, in the molecular beam. The coexistence of endohedral (not forming Ar complexes) and exohedral (forming Ar complexes) structures in the cluster beam, instead, is not excluded because the fraction of Ar complexes observed for $Si_{11}V^+$ is a lot smaller than the fraction of Ar complexes for Si_nV^+ with $n < 11$ (see ref 43). On the other hand, endohedral structures, such as **iso1**, are not expected to contribute to the measured absorption spectrum, as they do not attach Ar. Therefore, even if **iso1** would be the ground-state structure, its absorption spectrum would not be observed in the current experiment.

iso1 consists of a V atom encapsulated by a silicon cage of 11 atoms. As a consequence, this isomer is quite compact and does not show any high-frequency band as experimentally observed. The observed spectrum must come from some isomers possessing a more exposed V atom. Among many basketlike low-lying isomers, **iso8**, which is 0.78 eV higher than the lowest-energy isomer, seems to have more features fitting with the experimental data. **iso8** with a C_s symmetry is formed by substituting the highest-coordinated Si atom in a hexacapped trigonal prism and has a coordination number of eight. Its highest vibrational mode A′, located at 486 cm^{-1}, describes a symmetric stretching of the trigonal Si_4-pyramid on the top of the trigonal prism.

Other V-exposed isomers, energetically lower than **iso8**, are built up by adding Si onto the smaller Si_nV^+ clusters. For example, **iso3** and **iso7** are constructed by adding two Si atoms on the ground-state structure of Si_9V^+. Actually, many similar structures can be located in the same way. However, no single IR spectrum of the lower-lying isomers reproduces the experimental one satisfyingly.

4.2.18. $Si_{11}Cu^+$. Also for the Cu-doped cluster the quality of the IR-MPD spectrum is not as good as for the smaller sizes. However, we can see that it is characterized by some intense bands in the region from 425 to 500 cm^{-1}, and also one at around 275 cm^{-1}. The lowest-energy structure **iso1**, which is derived by substituting a Si by Cu in the hexacapped trigonal prism Si_{12}^+ (an isomer located in this work and lying 0.04 eV above the ground-state structure in ref 26), reproduces some experimental features in the 400−500 cm^{-1} range. However, the intensities of the bands centered at 275 cm^{-1} and the highest-energy band appear too low in its computed IR spectrum. The third lowest-energy isomer **iso3**, which lies 0.27 eV higher than **iso1**, matches the experimental data somewhat better. In this isomer, Cu adds to an edge of the pentacapped trigonal prism ground state structure of both Si_{11} and Si_{11}^+.[10,12,42] The highest-frequency band at 486 cm^{-1} arises from a symmetric stretch of a Si_4-pyramid farthest away from Cu. This frequency coincides

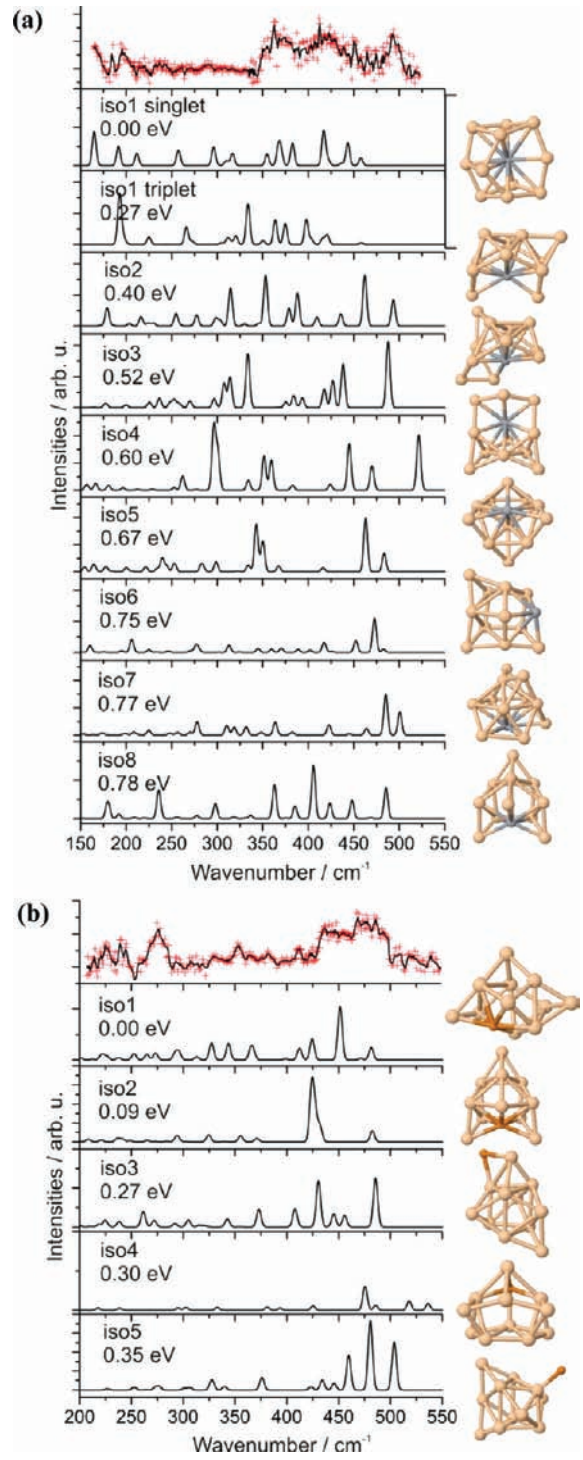

Figure 9. The upmost panel shows the experimental IR-MPD spectrum of $Si_{11}M^+ \cdot Ar$. Lower panels show the calculated IR spectra for some low-lying minima of $Si_{11}M^+$. (a) M = V; (b) M = Cu.

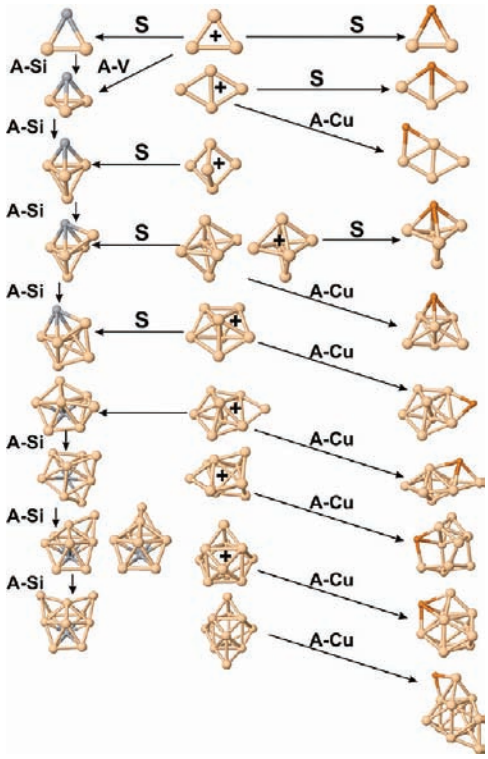

Figure 10. Growth mechanisms of the vanadium (left)- and copper (right)-doped silicon clusters in comparison with the bare silicon clusters (middle). **A-Cu**, **A-V**, and **A-Si** stand for the adsorption of a copper, vanadium, and silicon atom. **S** stands for the substitution. The sign "+" stands for the cationic bare silicon clusters. Structures of the neutral and cationic bare silicon clusters are from refs 10, 12, and 42.

with the highest-energy band of **iso8** of $Si_{11}V^+$, and they both originate from the same type of vibration. The next two lower-intensity bands come from the stretching vibrations of Si−Si bonds, which directly connect to Cu. The following intense band is an asymmetric vibration whose symmetric counterpart induces the highest-frequency band. Also in this case, it appears difficult to definitely assign the structure of $Si_{11}Cu^+$ based on the comparison of the presented spectra.

4.2.19. Overview of IR Spectra of V- and Cu-Doped Silicon Clusters. In general, the IR spectra are dominated by bands, which are mainly related to motions of Si_n moieties, while modes involving movements of the dopants often lead to less prominent features. Localized vibrations of moieties, such as the dimer Si_2, triangle Si_3, rhombus Si_4, and trigonal pyramid Si_4, often lead to bands at high frequencies. The pentagonal bipyramid building block has rather low-energy fundamental frequencies because it is compact, and its normal modes are strongly delocalized. However, the frequencies become higher in energy when there are additional Si atoms adsorbed on it, as the fundamental modes invariably include movements of the capped Si atoms.

4.3. Growth Mechanism of the Doped Clusters. Figure 10 gives an overview of the structures that we have discussed above for the cationic clusters Si_nV^+ ($n = 2-10$) and Si_nCu^+ ($n = 2-11$). It is obvious that, in singly doped silicon clusters, the V and Cu atoms change the geometries of the bare silicon clusters in different directions.

Most structures are assigned upon comparison of the computed and the experimental IR spectra. However, for the smallest sizes (Si_nM^+ with $n = 2, 3$ for M = V, and $n = 2-5$ for M = Cu), no experimental data was available, and for some of the larger sizes (Si_nM^+ with $n = 5, 9, 10$ for M = V, and $n = 9-11$ for M = Cu), no definite assignment could be made due to the limited quality of the experimental data. For these cases, the computed lowest energy isomer is retained in Figure 10. Exceptions are Si_9Cu^+, $Si_{10}V^+$, and $Si_{11}Cu^+$, for which an energetically higher lying isomer is given in Figure 10, because the BP86-based ground-state isomer was excluded on the basis of the experimental data.

Starting with $n = 2$, both doped silicon clusters have the same triangular shape. The third Si atom is added to Si_2V^+ to form a trigonal pyramid (**iso1**) as the ground state of Si_3V^+, whereas it bridges Cu and a Si atom on the molecular plane to generate the lowest-lying planar structure **iso1** of Si_3Cu^+. $n = 3$ is the only size where the V atom adsorbs to the bare cluster Si_3^+, while the Cu atom substitutes to the rhombus Si_4^+ to form Si_3Cu^+.

Cu keeps the doped silicon clusters planar up to $n = 4$ at which size the bare silicon cluster is also planar, whereas Si_4V^+ clusters already favor 3D structures. Comparison with the bare clusters shows that Si_4Cu^+ is an adsorptive derivative of the rhombus Si_4^+,[10,12] while Si_4V^+ is a substitutive derivative of the trigonal bipyramid Si_5^+.[10,12]

$n = 5$ is the size at which both dopants modify the bare silicon cluster in a similar way. In particular, both transition metal atoms substitute a Si atom at the axial position of the fluxional Si_6 leading to slightly different structures. While Si_5V^+ has a shape analogous to the neutral Si_6, Si_5Cu^+ has a shape similar to that of the bare cation Si_6^+.[36]

The structure **iso2** assigned to Si_6V^+ results from a substitution of a Si atom by V at an equatorial position of the pentagonal bipyramid Si_7^+ [42] and is calculated to be only 0.03 eV above the lowest-energy isomer **iso1**. From Si_7V^+ to $Si_{10}V^+$, V occupies an apex of the pentagonal bipyramid. There also exists an obvious growing path as the size of the cluster increases. Indeed, Si_8V^+ is obtained by adding one more Si atom to a Si−Si−V face of Si_7V^+. A consecutive addition of the ninth Si atom to the adjacent Si−Si−V face builds up Si_9V^+. An extra Si atom is added to a Si−Si−Si face of Si_9V^+ to result in the best fitting isomer of $Si_{10}V^+$ (**iso8**) that is, however, 0.18 eV higher in energy than the ground state.

For $n = 6-11$, the single Cu cation or Cu atom prefers to cap a face or an edge of the ground state structure of the bare Si_n or Si_n^+, respectively, leading to Si_nCu^+. The Mulliken charge distribution helps to reveal how the Cu and silicon framework combine to form Si_nCu^+. In particular, Si_6Cu^+ is formed by adding Cu to a face of the distorted octahedron Si_6^+ (ref 36) (the net charge on Si_6 is +0.76 *e*, *e* stands for the elemental charge). Si_9Cu^+ is formed by adding Cu to a face of the bicapped pentagonal bipyramid Si_9^+ (ref 42) (the net charge on Si_9 is +0.65 *e*) but the structure is strongly distorted. Si_7Cu^+ is formed by adding Cu to an equatorial edge of the pentagonal bipyramid Si_7^+ (ref 42) (the net charge on Si_7 is +0.48 *e*) and $Si_{11}Cu^+$ is produced by adding Cu^+ to an edge of the pentacapped trigonal prism Si_{11} (the net charge on Si_{11} is −0.18 *e*). In Si_8Cu^+ and $Si_{10}Cu^+$, the Cu atom is added on an edge and also bridges two apexes of the cationic bare clusters, namely the monocapped pentagonal bipyramid Si_8^+ and tetracapped trigonal prism Si_{10}^+ (ref 42). Although the isomers assigned in this study do not always correspond to the calculated lowest-energy isomers, they interestingly are all formed upon the adsorptions of Cu to the bare silicon clusters.

Nevertheless, the relative energies of the assigned isomers are just within the expected error bars of DFT methods (~0.3 eV) except for $Si_{11}V^+$. This means that the fitting isomer could

Table 1. HOMO−LUMO Gaps (H-L, eV), Average Binding Energy (E_b, eV), and Fragmentation Energies (D, eV) of the V- and Cu-Doped Silicon Clusters Shown in Figure 10[a]

	Si_nV^+, BP86			Si_nV^+, B3LYP			Si_nCu^+, BP86			Si_nCu^+, B3LYP		
n	H-L	E_b	*D*	H-L	E_b	*D*	H-L	E_b	*D*	H-L	E_b	*D*
2	0.81	2.40	3.82 (D_1)	2.65	1.98	2.89 (D_1)	1.00	2.42	3.54 (D_2)	2.24	2.11	3.13 (D_2)
3	1.17	2.83	3.90 (D_1)	2.69	2.33	2.61 (D_1)	1.43	2.77	3.55 (D_2)	2.49	2.41	2.95 (D_1)
4	1.66	3.06	3.37 (D_1)	2.82	2.44	1.33 (D_1)	1.34	3.07	3.04 (D_2)	2.60	2.76	2.74 (D_2)
5	0.79	3.24	3.60 (D_1)	2.48	2.70	2.01 (D_1)	2.04	3.28	3.71 (D_2)	3.13	2.89	3.12 (D_2)
6	0.76	3.37	3.61 (D_1)	2.17	2.94	2.57 (D_1)	1.24	3.37	2.92 (D_2)	2.66	3.00	2.52 (D_2)
7	1.05	3.44	3.35 (D_1)	2.63	2.93	1.73 (D_1)	2.14	3.50	3.30 (D_2)	3.30	3.12	2.93 (D_2)
8	1.14	3.51	4.06 (D_3)	2.57	2.99	2.76 (D_1)	1.26	3.45	2.78 (D_2)	2.23	3.05	2.19 (D_2)
9	0.96	3.56	3.97 (D_3)	2.24	3.04	2.56 (D_1)	1.78	3.52	3.13 (D_2)	2.80	3.12	2.72 (D_2)
10	0.86	3.55	3.36 (D_1)	1.94	3.04	1.70 (D_1)	2.18	3.60	3.35 (D_2)	3.28	3.18	2.81 (D_2)
11							0.94	3.56	2.45 (D_2)	1.98	3.16	2.12 (D_2)

[a] For the fragmentation energies the most facile pathway (D_1, D_2, or D_3) is given; this path is listed between brackets. The parameters are calculated using the BP86 and B3LYP functionals.

be the real ground state if more accurate computational levels could be applied. Irrespective of the relative ordering, the fitting isomers are always in a good agreement with the growth mechanism of each series.

In general, V prefers a substitution to a high-coordinated position of the cationic bare silicon clusters, whereas Cu favors an adsorption to the neutral or cationic bare clusters and a lower coordination number. The pentagonal bipyramid remains an essential structural motif in the exohedral-doped silicon clusters. Indeed, Si_7Cu^+, Si_8Cu^+, and Si_9Cu^+ retain the pentagonal bipyramid Si_7^+. For Si_nV^+, the pentagonal bipyramid motif starts at $n = 6$ where V takes an equatorial position of Si_7^+. For $n = 7-10$, V occupies a top of one pyramid side. The transition from a pentagonal bipyramid motif to a trigonal prism seems to occur at $n = 10$ for the Cu-doped clusters, and at $n = 11$ for the V-doped clusters. The calculated lowest-lying isomer of $Si_{11}V^+$ is a cage structure, but the results of an earlier argon physisorption experiment demonstrated that exohedrally doped $Si_{11}V^+$ must exist in the molecular beam.[43] These findings indicate that possibly both an exohedral and an endohedral isomer coexist in the experiment. It is somewhat surprising that the transition from exohedral to endohedral structures for Cu- and V-doped silicon clusters happens at similar sizes, although their structures follow different growth patterns.

Investigating the natural electronic configurations of each atom in the molecule using the NBO 3.1 program,[69] we find that the number of electrons in 3d orbitals of Cu is always around 9.8 electrons, whereas in the case of doping with V, it varies and especially increases with cluster size from $n = 6$ (3.3) to $n = 11$ (5.6) (see Table S1 of the Supporting Information). These results indicate that the V atom plays the role of an acceptor due to the unfilled 3d orbitals; thus, it is easier to have a high-coordination number by substituting to an appropriate position. In contrast, Cu favors a low coordination number and thus simply adds to the bare Si clusters, due to its fully occupied 3d orbitals.

4.4. Energetic Stabilities. To further understand the stability of the transition metal-doped silicon clusters, Si_nM^+ (M = Cu, V), the average binding energies, $E_b(n)$, and fragmentation energies for several pathways were evaluated. The fragmentation by losing M^+ (D_1), M (D_2), and a neutral Si atom (D_3) are considered. It should be noted that dissociation channels involving larger fragments might be competing in energy with D_1, D_2, and D_3, because Si_4, Si_6, Si_7, and Si_{10} are found as frequent fragmentation products for several bare silicon clusters.[70] The following formulas are used:

$$E_b(n) = [E(M^+) + nE(Si) - E(Si_nM^+)]/(n + 1)$$

$$D_1 = E(Si_n, \text{lowest isomer}) + E(M^+) - E(Si_nM^+)$$

$$D_2 = E(Si_n^+, \text{lowest isomer}) + E(M) - E(Si_nM^+)$$

$$D_3 = E(Si_{n-1}M^+) + E(Si) - E(Si_nM^+)$$

The total energy of the assigned isomers is calculated using the BP86 and B3LYP functionals. The $E_b(n)$, HOMO−LUMO gap, and the fragmentation energy for the most facile channel are summarized in Table 1. The HOMO−LUMO gaps calculated by B3LYP are systematically higher than BP86, which is in line with previous studies.[65] Both B3LYP and BP86 show that the Si_nV^+ clusters dissociate by losing the vanadium cation, with exception of Si_8V^+ and Si_9V^+ for which neutral Si loss is favored according to BP86. On the other hand, Si_nCu^+ prefers to dissociate by loss of neutral Cu. The difference between Si_nV^+ and Si_nCu^+ is related to the lower ionization energy of the V atom (6.74 eV) with respect to the Cu atom (7.73 eV).

Analysis of the size dependence of E_b and the dissociation energies points out that Si_8V^+ and Si_9V^+ are somewhat more stable than the other Si_nV^+ sizes. Unfortunately, there are no experimental results to compare. For Si_nCu^+, fragmentation studies showed an enhanced stability for Si_6Cu^+, Si_7Cu^+, and $Si_{10}Cu^+$.[23,31] The calculated energetic properties (HOMO−LUMO gap, E_b, and dissociation energies) confirm this enhanced stability for Si_7Cu^+ and $Si_{10}Cu^+$ at BP86 as well as B3LYP level of theory. For Si_6Cu^+ our evidence is less clear, Si_6Cu^+ has a higher E_b than that of all smaller clusters but is clearly less stable than Si_7Cu^+ given the considered fragmentation pathways. It is known that silicon clusters also dissociate by losing large fragments.[70] Therefore, we analyzed all different fragmentation channels for $Si_{10}Cu^+$. According to B3LYP, the most facile pathways then are the loss of Cu (2.81 eV), the loss of Si_4 (3.10 eV), and the loss of Cu^+ (3.22 eV). BP86 predicts the loss of Cu (3.35 eV) and the loss of Cu^+ (3.94 eV). All other fragmentation paths require more than 4 eV. Fragmentation experiments on $Si_{10}Cu^+$ showed that the loss of Si_4 (and thus the creation of Si_6Cu^+) is a favorable channel.[31] This demon-

(69) Glendening, E. D.; Reed, A. E.; Carpenter, J. E.; Weinhold, F. NBO Version 3.1.

(70) Qin, W.; Lu, W. C.; Zhao, L. Z.; Zang, Q. J.; Wang, C. Z.; Ho, K. M. *J. Phys.: Condens. Matter* **2009**, *21*, 455501.

strates that B3LYP performs better than BP86 when predicting fragmentation paths.

5. Concluding Remarks

The following conclusions emerge from the present combined experimental and computational study of transition metal-doped silicon clusters.

(i) In most cases, the structure of V- and Cu-doped silicon clusters produced in the molecular beam can be identified with high certainty. The overall good agreement between computed and experimental IR spectra indicates that the BP86 functional in combination with the 6-311+G(d) basis set is suited to predict vibrational parameters of these clusters.

(ii) The IR spectra hardly show characteristic features of the dopants, such as the "fingerprint bands" of functional groups, but they are dominated by modes related to Si_n moieties. Some moieties, such as the dimer Si_2, triangle Si_3, rhombus Si_4, and trigonal pyramid Si_4, often show high-energy IR absorptions.

(iii) In most cases, the calculated IR spectrum of the most stable structure can explain the experimental far-IR counterpart, which is measured on the corresponding $Si_nM^+ \cdot Ar$ complexes. The Ar is expected to attach to the metal atom of exohedral Si_nM^+ clusters. In a few cases, the best fitting isomer is not the lowest in energy but the energy difference ranges within the expected errors of the computational (DFT) methods. Irrespective of their relative energies, the assigned isomers follow the described growth pattern, in the cases of Si_6V^+, Si_9Cu^+, $Si_{11}Cu^+$, and $Si_{10}V^+$.

(iv) A clear picture of the disparate effects of the two dopants on the host silicon clusters has been shown. While V prefers to substitute at a high-coordinated position of the cationic bare silicon clusters, the Cu tends to adsorb to the bare clusters in a low coordinated site.

(v) The change from a basic pentagonal bipyramid motif to a trigonal prism appears to happen at $n = 10$ for the Cu dopant and at $n = 11$ for the V dopant. Theory predicts a cage structure as the lowest-lying isomer of $Si_{11}V^+$, which does not agree with the experimental absorption spectrum of $Si_{11}V^+ \cdot Ar$, as expected from our previous conclusion that Ar complex formation is a signature of exohedral isomers.

(vi) Although Cu and V show a similar behavior at the transition size from exohedral to endohedral structures, they are not following the same growth mechanism.

(vii) The relative stability of the clusters is probed by the calculated energetic parameters using the BP86 and B3LYP functionals. The differences between the Cu- and V-doped Si clusters stem from the different numbers of the empty 3d-orbitals of the dopants.

Acknowledgment. We gratefully acknowledge the support of the Stichting voor Fundamenteel Onderzoek der Materie (FOM) in providing beam time on FELIX. The authors thank the FELIX staff for their skillful assistance, in particular Dr. B. Redlich and Dr. A. F. G. van der Meer. The research leading to these results has received funding from the European Community's Seventh Framework Programme (FP7/2007-2013) under grant agreement no. 226716 (ELISA). The Leuven groups acknowledge support by the Research Foundation - Flanders (FWO), the Flemish Concerted Action (GOA), and the Belgian Interuniversity Poles of Attraction (IAP) research programs. P.G. thanks the IMPRS: Complex Surfaces in Materials Science for funding, and P.C. the Institute for the Promotion of Innovation by Science and Technology in Flanders (IWT) for financial support.

Supporting Information Available: Complete ref 66; the natural electronic configurations of the transition metal atom in the doped silicon clusters; comparison of calculated IR spectra for the Ar-free clusters and the corresponding Ar−cluster complexes of Si_6V^+ and Si_6Cu^+; comparison of calculated IR spectra using the BP86 and B3LYP functionals for Si_6Cu^+ and Si_7Cu^+; structures of more low-lying isomers and the optimized coordinates of some selected isomers at sizes $n = 4-11$ together with their absolute energies in hartrees. This material is available free of charge via the Internet at http://pubs.acs.org.

JA105099U